AD-A037 347 BALLISTIC RESEARCH LABS ABERDEEN PROVING GROUND MD F/G 20/4
SEPARATION AHEAD OF PROTUBERANCES IN SUPERSONIC TURBULENT BOUND--ETC(U)
FEB 77 R SEDNEY, C W KITCHENS

UNCLASSIFIED BRL-1958 NL

1 OF 1
AD A037347

END

DATE FILMED
4-77

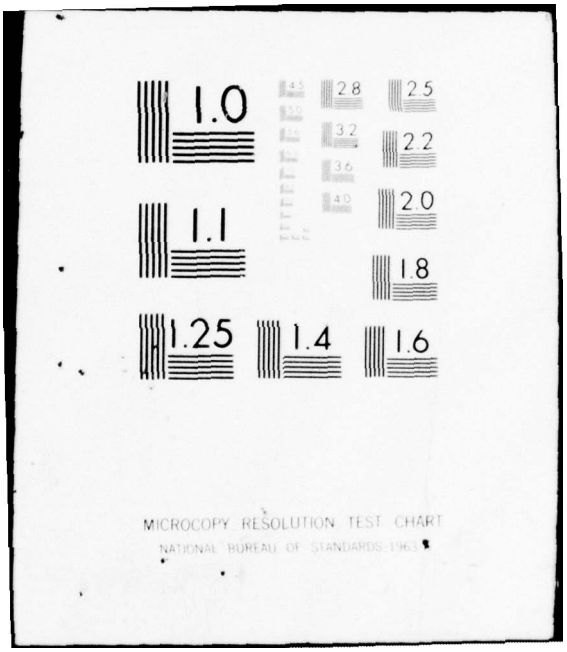
1.0
1.1
1.25
1.4
1.6
2.8
2.5
3.2
2.2
3.6
2.0
4.0
1.8
MICROCOPY RESOLUTION TEST CHART
NATIONAL BUREAU OF STANDARDS 1963

BRL

AD

REPORT NO. 1958

SEPARATION AHEAD OF PROTUBERANCES IN SUPERSONIC TURBULENT BOUNDARY LAYERS

Raymond Sedney
Clarence W. Kitchens, Jr.

February 1977

USA BALLISTIC RESEARCH LABORATORY
ABERDEEN PROVING GROUND, MARYLAND

Destroy this report when it is no longer needed.
Do not return it to the originator.

Secondary distribution of this report by originating or sponsoring activity is prohibited.

Additional copies of this report may be obtained from the National Technical Information Service, U.S. Department of Commerce, Springfield, Virginia 22151.

The findings in this report are not to be construed as an official Department of the Army position, unless so designated by other authorized documents.

UNCLASSIFIED

SECURITY CLASSIFICATION OF THIS PAGE (When Data Entered)

REPORT DOCUMENTATION PAGE

READ INSTRUCTIONS BEFORE COMPLETING FORM

1. REPORT NUMBER: REPORT NO. 1958
2. GOVT ACCESSION NO.
3. RECIPIENT'S CATALOG NUMBER

4. TITLE (and Subtitle): Separation Ahead of Protuberances in Supersonic Turbulent Boundary Layers.
5. TYPE OF REPORT & PERIOD COVERED: Final Sept.,
6. PERFORMING ORG. REPORT NUMBER

7. AUTHOR(s): Raymond Sedney, Clarence W. Kitchens, Jr.
8. CONTRACT OR GRANT NUMBER(s): 1T161101A91A

9. PERFORMING ORGANIZATION NAME AND ADDRESS: USA Ballistic Research Laboratory, Aberdeen Proving Ground, Maryland 21005
10. PROGRAM ELEMENT, PROJECT, TASK AREA & WORK UNIT NUMBERS

11. CONTROLLING OFFICE NAME AND ADDRESS: US Army Materiel Development & Readiness Command, 5001 Eisenhower Avenue, Alexandria, VA 22333
12. REPORT DATE: FEBRUARY 1977
13. NUMBER OF PAGES: 37

14. MONITORING AGENCY NAME & ADDRESS (if different from Controlling Office): BRL-1958
15. SECURITY CLASS. (of this report): UNCLASSIFIED
15a. DECLASSIFICATION/DOWNGRADING SCHEDULE

16. DISTRIBUTION STATEMENT (of this Report)

Approved for public release; distribution unlimited.

17. DISTRIBUTION STATEMENT (of the abstract entered in Block 20, if different from Report)

18. SUPPLEMENTARY NOTES

19. KEY WORDS (Continue on reverse side if necessary and identify by block number)

Separation	Primary Separation	Obstacles
Protuberances	Flow Visualization	Correlation
Fluid Dynamics	Optical-Surface Indicator	Supersonic
Turbulent Boundary Layer		

20. ABSTRACT (Continue on reverse side if necessary and identify by block number)

The data were obtained using the optical-surface indicator technique of visualizing the flow; its accuracy and reproducibility are discussed. The protuberances are immersed in the boundary layer on the wall of a supersonic wind tunnel. The relative importance of various non-dimensional groups is evaluated. The variation of primary separation distance is presented as a function of obstacle dimensions, Mach number, and Reynolds number, the last being the least significant. These results do not support some scaling laws found in the literature. An alternative correlation is proposed which applies to both small and large cylindrical protuberances.

DD FORM 1 JAN 73 1473 EDITION OF 1 NOV 65 IS OBSOLETE

UNCLASSIFIED

SECURITY CLASSIFICATION OF THIS PAGE (When Data Entered)

050 750

TABLE OF CONTENTS

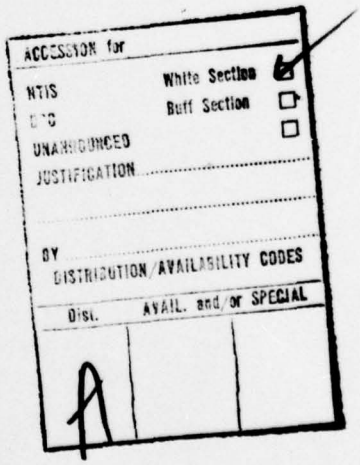

LIST OF ILLUSTRATIONS

I. INTRODUCTION

Although aerodynamic vehicles are usually designed as smooth, streamlined shapes, the production version will often have protuberances on the surfaces. If a protuberance is relatively blunt then the boundary layer will separate and a strong interaction between the viscous and inviscid flows results. If it is highly swept or has a sharp leading edge, separation with weak interaction can be obtained. It is convenient to distinguish small and large protuberances on the basis of their height, k, relative to the 99% velocity boundary-layer thickness, δ. For a given bluntness the extent of separation is greater the larger the protuberance, although the asymptotic result is obtained rather quickly for $k > \delta$. The extent of separation near the obstacle is of interest because of its relation to the pressure, heat transfer, and skin friction distributions in the separated flow. The first object of this paper is to present measurements obtained by flow visualization techniques of the extent of separation ahead of protuberances immersed in a supersonic turbulent boundary layer. The second is to discuss correlations of these data. Since the conclusions depend on the reliability of these data, an ancillary objective is to evaluate the optical-surface indicator technique.

For small protuberances a number of features in the flow can be described in terms of vortex systems. A survey of the effects of small protuberances on boundary-layer flows[1] shows that these features are common to a wide range of conditions: for both laminar and turbulent boundary layers and for all speeds up to hypersonic. However, a more detailed examination of the flow structure is lacking except for laminar, low speed flow. A discussion of several details of the structure for turbulent, high speed flow is given in Reference 2. The flow structure is needed not only to achieve an intuitive understanding of the flow but also to give some insight into the pressure, heat transfer and shear distributions near and on the protuberance.

Data on pressure and/or heat transfer are available in many references, mostly for large protuberances. These are discussed in

---

1. R. Sedney, "A Survey of the Effects of Small Protuberances on Boundary Layer Flows," AIAA Journal, Vol. 11, No. 6, June 1973, pp. 782-792.

2. R. Sedney and C. W. Kitchens, Jr., "The Structure of Three-Dimensional Separated Flows in Obstacle-Boundary Layer Interactions," AGARD-CP-168, Flow Separation, Paper 37, pp. 1-15. See also BRL Report 1791, Ballistic Research Laboratories, June 1975 (AD A011254).

Reference 1, the survey by Korkegi[3] and the report by Kaufmann et al[4]. The very high values of pressure, pressure gradient and heat transfer measured on and in the vicinity of large protuberances in supersonic flow are remarkable aspects of this separated flow. Such high values are not found in the relatively few experiments with small protuberances.

Understanding the flow structure and correlating the vast amount of data available are made difficult by the number of parameters that must be considered. The dimensions (three lengths), shape and orientation (sweep) of the obstacle are important. The undisturbed velocity profiles (laminar or turbulent, 2-D or 3-D) and δ must be considered as well as Mach number, M, and the Reynolds numbers that can be formed with the various lengths. The undisturbed velocity, U_k, at the height k off the surface has been found important in low speed flows. Heat and mass transfer and turbulent shear should be considered but we are unaware of any experiments which systematically vary these. This plethora of parameters is relieved somewhat for large protuberances; if $k > \delta$ and the width is small compared to δ, then the height no longer influences the flow interactions. In view of the large number of parameters even partial success at correlating important flow features will be helpful.

A correlation for cylindrical obstacles was proposed by Westkaemper[5], using a large collection of data on primary separation distance, S. This is defined as the distance from the leading edge of the obstacle to the most upstream location of separation. His correlation was proposed for cylinders of diameter D with $k > \delta$ over the Mach number range $2 \leq M \leq 20$ and for all Reynolds numbers provided the boundary layer is turbulent. Unfortunately, as more data become available, the deviation of the data from this correlation increases. A critique of this correlation is presented.

A correlation is proposed here, for large and small cylindrical obstacles, using the separation distance data obtained from the

---

3. R. H. Korkegi, "Survey of Viscous Interaction Associated with High Mach Number Flight," AIAA Journal, Vol. 9, No. 5, May 1971, pp. 771-784.

4. L. G. Kaufman, R. H. Korkegi and L. C. Morton, "Shock Impingement Caused by Boundary-Layer Separation Ahead of Blunt Fins," AIAA Journal, Vol. 11, No. 10, October 1973, pp. 1363-1364. See also ARL 72-0118, Aerospace Research Laboratories, August 1972.

5. J. C. Westkaemper, "Turbulent Boundary-Layer Separation Ahead of Cylinders," AIAA Journal, Vol. 6, No. 7, July 1968, pp. 1352-1355.

optical-surface indicator technique[6,7], which is particularly suited to this application; it yields a vast amount of detailed information about the surface flow pattern[2]. The flow implied by these patterns can be related to some of the trends in the data for S. Westkaemper concluded that S/D is strongly dependent on k/D and only weakly dependent on Reynolds number. Our results support these two conclusions, but also show a significant dependence on M. The correlation is more successful for large cylinders since S scales with D; this is not true for small cylinders.

II. DESCRIPTION OF THE EXPERIMENT

The experiments were conducted in a continuous, supersonic wind tunnel at the Ballistic Research Laboratories. The dimensions of the test section are 33 x 38 cm. The interactions were studied by placing the protuberances in the wall boundary layer, having a typical thickness of 2.5 cm at M = 2.50. The optical-surface indicator technique requires mounting the obstacle on a tunnel window. Obtaining side-view shadowgraph and schlieren pictures, which show the trace of the shock surfaces, requires placing the obstacle on the floor (or ceiling) of the tunnel. Velocity profiles and integral boundary-layer thicknesses for the floor and sidewall boundary layers are presented in Reference 8. The pitot pressure data were taken with no protuberance in the flow, at the point where the center of the protuberance would be mounted. The boundary layers were not surveyed off the centerline. The only measure of the transverse uniformity of the sidewall boundary layer was obtained by visualizing the separation line in the flow over a bar model; this line was straight over a length of at least 10cm, even without optimum side plates. Figure 1 shows δ as a function of unit Reynolds number, R/ℓ, and M for both boundary layers. On the basis of skin friction estimates we conclude that both boundary layers are fully-developed turbulent boundary layers at all test conditions, except possibly for the floor boundary layer at the lowest R/ℓ at M = 3.50 and 4.50; the floor boundary layer is not used for determining separation.

---

6. R. Sedney, "Visualization of Boundary Layer Flow Patterns Around Protuberances Using an Optical-Surface Indicator Technique," The Physics of Fluids, Vol. 15, No. 12, December 1972, pp. 2439-2441.

7. R. Sedney, C. W. Kitchens, Jr., and C. C. Bush, "Combined Flow Visualization Techniques," AIAA Paper 76-55, AIAA 14th Aerospace Sciences Meeting, Washington, DC, January 1976.

8. C. W. Kitchens, Jr., C. C. Bush and R. Sedney, "Characteristics of the Sidewall and Floor Boundary Layers in BRL Supersonic Wind Tunnel No. 1," BRL Memorandum Report 2563, Ballistic Research Laboratories, December 1975 (AD B008566L).

A brief description of the optical-surface indicator technique will be given; for more details see References 6 and 7. The obstacle is mounted on a test section window using a bolt and seal. Figure 2 shows a schematic view of the experimental set-up and a sketch of some features of the flow over a small protuberance. A small amount of lightweight, transparent oil is placed on the window before and/or after the flow is started. After the surface flow pattern is established, typically in one minute, a shadowgraph or schlieren picture is taken. These plan-view pictures show the surface (window) flow pattern and parts of the shock surfaces. An example is shown in Figure 3. The relation between the streaks and flow near the surface is discussed in Reference 9. Schlieren pictures are taken by flashing a BH-6 tube. The schlieren light source and one parabolic mirror are used for continuous viewing on a frosty mylar screen. Shadowgraphs are taken with a spark light source of 1 μs duration.

Several methods of introducing oil onto the window are used; in this way the prominence of particular features of the surface flow pattern can be selectively increased. Usually a regular array of oil drops and/or droplets from a spray of light machine oil are used. The clearest definition of the surface flow pattern is obtained when the oil drops are drawn out into streaks of height 0.1 mm or less. The intensity of the image of the streak is then about 50% of the undisturbed intensity; it appears gray. If the cross-section of the streak is such that it is almost opaque, the spacing must be considerably greater to obtain a clear pattern, decreasing the resolution. The observed variation in intensity can be predicted approximately by geometrical optics calculation[7].

In Figure 3 most of the streaks are gray. Several prominent features are labeled. The attachment line A is difficult to see in a reproduction unless the region is enlarged, see References 1 and 7 for examples. If oil is placed near and upstream of the protuberance before flow is started, it is mostly wiped away by the time a shadowgraph is taken. Oil can be introduced through a pressure tap upstream of the window after flow is established to obtain a clear image of A which lasts for a few minutes. This is the region of highest shear and, from the results of other investigators, e.g., Reference 10, highest heat transfer. As in all shadowgraphs, a shock wave surface will produce a shadow only if there are light rays at nearly grazing incidence to the surface. Since the cylinder in Figure 3 is a large protuberance, the

---

9. R. L. Maltby, "Flow Visualization in Wind Tunnels Using Indicators," AGARD-ograph 70, AGARD-NATO Fluid Dynamics Panel, 1962.

10. E. A. Price and R. L. Stallings, "Investigation of Turbulent Separated Flows in the Vicinity of Fin-Type Protuberances at Supersonic Mach Numbers," NASA TN D-3804, February 1967.

shock pattern is not like the side view sketched in Figure 2 but consists of a bow shock which intersects a separation shock, well below the top of the cylinder, resulting in a Mach stem plus other complex structure. The leading edge of the bow shock will be almost parallel to the cylinder axis for some extent. Thus the light rays (see Figure 2) will be at almost grazing incidence and the prominent shadow shown in Figure 3 results.

For the conditions of Figure 3, the bow shock is steady and hence has a distinct shadow; the unsteadiness of the Mach stem explains its irregular shadow. This unsteadiness is shown in our side-view shadowgraphs and has been found by other investigators. The dominant frequency of the oscillation, from other kinds of shock intersection studies, is probably on the order of 1000 Hz. The shear at the wall, which forms the surface flow pattern, has a dominant frequency which is presumed to be much less. Suffice it to say a surface indicator method can only give a representation of an average flow pattern.

Since primary separation is of main concern here it is fortunate that a well-defined image of the primary separation line can be obtained consistently with relative ease. If a spray is used, a ragged pattern can result if some droplets are deposited very near the position of primary separation. The small droplets from the spray are influenced by flow irregularities in the tunnel starting process and afterwards there is insufficient shear force to change the pattern once steady flow is established. A clearly defined separation line can be obscured if too much oil is introduced through the upstream pressure tap. In the next section the accuracy of the measurement of S is discussed.

Different flow visualization methods were used to examine other aspects of the flow: two surface indicator methods were used to obtain the flow pattern on the protuberances; conventional, side-view shadowgraph and schlieren methods provided the trace of the shock surfaces and an indication of the boundary-layer edge; the vapor screen method visualized the shock surfaces and some of the vortices. The results from these are not pertinent to this discussion of primary separation; they are available in Reference 2.

Data were taken at M = 1.5, 2.5, 3.5, 4.0, and 4.5, but mostly at M = 2.5 and 3.5. The stagnation temperature was nominally 306°K. The stagnation pressure, p_o, or unit Reynolds number, was varied over the allowable limits which are shown by the values in Figure 1. Most of the data were obtained by setting the tunnel to operate at the desired p_o. The same separation pattern could be obtained by starting at a lower p_o and increasing it to the desired value. However, decreasing p_o to the desired value gave a poorly defined pattern.

The experiments were performed using obstacles of simple geometrical shape: circular cylinder, hemisphere, parallelepiped, truncated cone, and bar. The bar was used mainly in a study of side plate design. It also provided the information on transverse flow uniformity mentioned earlier. Table 1 gives the dimensions of the models, the notation used in referring to them (e.g., 2C), and the symbols used when plotting results for several cylinders on the same figure.

III. PRIMARY SEPARATION

The upstream extent of the separated flow is bounded by a curve called the primary separation line. We define the distance, in the free stream direction, from the leading edge of the obstacle to the primary separation line to be S, the primary separation distance. Although the complete primary separation line upstream of the body is easily determined from our plan-view shadowgraphs, only results for S will be presented. Because we simultaneously visualize the bow shock, correlation of it with the primary separation line is straightforward. The measured bow shock detachment distances for models 1D and 2D agree with those in the literature for two-dimensional flow over cylinders to within 5%.

A question arises as to how separation is defined from experimental measurements. In the literature it has been defined by means of pressure or heat transfer distributions, side-view schlieren or shadowgraph photographs, or surface indicator techniques. The fact that these give different results has been discussed in the literature (especially for two-dimensional flows); we will not elaborate on this. Note that Price and Stallings[10] make a distinction between the disturbed flow region, as determined by pressure measurements, for example, and the separated flow region, as determined by surface indicators. General use of such a convention would obviate confusion. Unsteady effects, which certainly exist in the flow, will affect the experimental definition of separation in different ways for the various measurement techniques. The surface-indicator technique, with its extremely slow response time, gives an indication of an average surface flow pattern that is clear and repeatable. Unsteadiness in flows of the type considered here is discussed in Reference 4 with respect to static pressure measurements; they conclude that their pressure distributions are not repeatable.

Only a very small amount of oil is required in the optical surface-indicator technique, as little as $0.05 cm^3$ being enough to obtain some of the complete surface patterns. The height of the oil accumulation line in a pattern, such as that shown in Figure 3, is considerably less than 0.1mm. Therefore we expect the interaction of the oil with the separated flow and the displacement of the oil line from the primary separation line to be negligible. A more quantitative statement can be made after considering the order of magnitude of the three aerodynamic forces acting on the oil line. These are shear, drag, and buoyancy. The last

was used in Reference 11 to explain a spurious oil accumulation line. The shear force is independent of the height of the oil, h; drag is a linear function of h; and buoyancy is quadratic with h, being expressible as a product of h/δ and a Reynolds number based on h and wall quantities. For the values of h obtained in the optical-surface indicator technique buoyancy is of second order importance and drag is small to the first order in h, compared to shear, which is the quantity we wish to indicate by the oil line.

The accuracy of our measured values of S is ± 1% except at the lowest stagnation pressures for which it is ± 3%. These error bounds include effects from both repeatability of the pattern and reading accuracy. Additionally, there is a slight amount of geometrical magnification in the images on the shadowgraph because the light from the spark source is diverging. This systematic error has been accounted for. Most often the correction is negligible, but in some cases it amounts to 5% in the ratio S/D.

For cylinders S is a function of the following variables: D, k, δ, free stream velocity, U_k (for small protuberances), kinematic viscosity, sound velocity, density, and a measure of the turbulent shear. We have no measure of the turbulent shear and we find that U_k is not significant as an independent variable, so these are left out of the dimensional analysis. In terms of non-dimensional parameters

$$S/D = f(k/D,\ D/\delta,\ R_D,\ M) \quad ; \tag{1}$$

where R_D is the Reynolds number based on D and free stream velocity. Of course this can be written in other equivalent forms, so that, e.g., k/δ and R_k appear as two of the four non-dimensional parameters. It is often convenient to use the three ratios of lengths even though they are not independent. Likewise, three Reynolds numbers could be defined; we do not have enough points in parameter space to tell which of these is most meaningful. The variation of S/D with any of these Reynolds numbers is weak compared to the other three non-dimensional parameters.

Curves of S/D versus k/δ are given in Figure 4 to show the approach to the "infinite length" cylinder case. For each curve three of the four possible dimensionless parameters are constant, viz., D/δ, R_D, and M. From the data in the literature, and as expected, S/D approaches a constant as k/δ increases. The results in Figure 4 show that the rate

---

11. D. R. Chapman, D. M. Kuehn and H. K. Larson, "Investigation of Separated Flows in Supersonic and Subsonic Streams with Emphasis on the Effect of Transition," NACA Report 1356, 1958.

of approach to the asymptote depends on D/δ. A large protuberance can be defined by the requirement that S/D differs by some small fraction from the asymptotic value. Models 1D and 2D, with $k/\delta = 4.5$, are good approximations to large cylinders. Other definitions are possible, e.g., requiring two-dimensional flow on some portion of the cylinder. On that basis these models are not large[2]; a much larger k/δ would be needed. We shall adopt the definition based on S/D.

The same kind of conclusions are reached if the data for M = 3.5 are plotted in the manner of Figure 4. Instead these data are presented in Figure 5 with the roles of k/δ and D/δ interchanged. For models 1D and 2D, with $k/\delta = 3.69$, the variation of S/D with D/δ is only slightly larger than the estimated error in S/D. Thus these two data points, shown by the triangles, are consistent with the results of many other investigators, viz., that S/D is independent of D for large cylindrical protuberances. Contrast this with the results for small protuberances; e.g., S/D changes by more than a factor of 2 for $k/\delta = 0.37$. The simple and satisfying scaling law valid for large protuberances is not valid for small ones.

The integers which appear above each data point refer to the number of vortices found between the obstacle and primary separation[2]. We find there are 2, 4, or 6 vortices depending on Reynolds number. Although the variation of S with R_D is not very large, the complex structure within the separated pocket changes significantly. The overall structure in the separated flow upstream of the obstacle is now fairly clear but there are still some important details that must be clarified. The sensitivity of the number of vortices to changes in unit Reynolds number, R/ℓ, is an interesting fact for which we have no explanation at present.

Another conclusion reached in some other studies of separation caused by large, cylindrical obstacles is that S/D is weakly dependent on M. This dependence, for the large cylinders 1D and 2D, is shown in Figure 6. The variation in S/D is more than 50%. The data points are connected with straight lines as a reading aid. For the small protuberances a variation of S/D with M is established only for model 2B; but the trend of increasing S/D with M is clear for all models. Note that even though R/ℓ is constant, δ varies because M changes. Thus the change of S/D with M and k/D, shown in Figure 6, is affected by other parameters.

Data for S/D vs. k/D are presented in Figures 7 and 8 for M = 2.5 and 3.5 respectively. Since R/ℓ and M are fixed for each figure, δ is constant for each plot. It follows that neither k/δ nor D/δ is constant for all the points of Figure 7 or 8; points with constant k/δ or D/δ can be identified with the help of Table 1. The different values of S/D at a fixed k/D reflect variations in the other parameters and not scatter in the data. For example, at k/D = 1.06 in both Figures 7 and 8 the

values of k/δ, D/δ, and R_D differ by a factor of 2 for the two points. It is important to observe that the spread in the data points, especially for small protuberances, is smaller for the S/D vs. k/D plot than for the previous three figures. This observation provides a starting point for correlating the data. Figure 7 also shows two data points from Reference 4 and five from Reference 12 for M = 2.5 but for R/ℓ = 31×10^6/m and 132×10^6/m (sic) respectively. The points taken from Reference 12 are for cylinders of "infinite effective height"; they are indicated by an interval because the k/D values were unspecified. These values are 2.5% higher than those for models 1D and 2D. These data were obtained using surface indicator methods but no error estimates were given. At any rate there is substantial agreement between our data and those of References 4 and 12. The effect of large changes in k/δ can be deduced by comparing our data and those of Reference 4 wherein δ = 0.24cm, k/δ = 32, and $R_D \times 10^{-5}$ = 3 and 6 for the two points at k/D = 4 and 8 respectively. The differences in R_D between our data and those of Reference 4 give a negligible change in S/D. Thus, if k/D is large, S/D is independent of k/δ. This empirical conclusion can be considered valid only for the range of parameters of the data on which it is based.

In Figure 8 two points from Reference 4 are shown but for M = 3.0 and 4.0. The value of S/D for M = 3.0 is less than that for M = 2.5 in Reference 4 and the values of k/D are not much different; this inconsistency casts some doubt on the M = 3.0 data point. Our other data, at M = 1.5, 4.0, 4.5, are consistent with the trends shown in Figures 7 and 8. Another data point, based on surface indicator methods, can be obtained from Winkelman[13]. He deduced S/D = 2.5 from post-test photographs, but this value is uncertain because of a pronounced shift of the oil accumulation line at tunnel shutdown. The conditions are M = 5, k/D = 12.32, D/δ = 0.195, $R/\ell = 24.3 \times 10^6$ which are sufficiently different from ours to prevent a direct comparison. Extrapolation of our data to these conditions gives a difference of about 30%.

A discussion of the data of Westkaemper[5] is given in the next section. Here the data reported by Voitenko et al[12] are considered; this is one of the more comprehensive studies of separation caused by cylindrical obstacles. Results are given for M = 2.5 and only one, rather high, value of R/ℓ. Comparison of these with our data, in the most

---

12. D. M. Voitenko, A. I. Zubkov and Y. A. Panov, "Supersonic Gas Flow Past a Cylindrical Obstacle on a Plate," Mekhanika Zhidkosti i Gaza, Vol. 1, No. 1, 1966, pp. 121-125.

13. A. E. Winkelmann, "Flow Visualization Studies of a Fin Protuberance Partially Immersed in a Turbulent Boundary Layer at Mach 5," NOLTR 70-93, Naval Ordnance Laboratory, May 1970.

primitive form, is frustrated by a lack of certain information in Reference 12. In Figure 7 only the five data points for cylinders of "infinite effective height" were shown. The S data in Reference 12 for finite height cylinders are presented in the form S/S_∞ vs. k/D where S_∞ is the value of S for the "infinite effective height" cylinder of the same diameter. The data shown in Figure 7 were normalized in that way and replotted in Figure 9 together with the data of Reference 12. The value $S_\infty/D = 2.00$ from that reference was chosen rather than 1.95 as indicated by our data. Since values of k, D, and δ, or their ratios, are not given, further discussion of this comparison is unfruitful. The trends agree. It is implied in Reference 12 that the cylinder diameters for these points are not all the same. Note that by choosing points with different k and D values, a smooth curve could be drawn which lies close to that through the points of Reference 12.

Variations of S/D with Reynolds number are difficult to present because no consistent trends were observed. Furthermore to obtain a significant change in, say, R_D by changing D and also keeping the other dimensionless parameters approximately constant, would require many more models than we have used. Limitations of the wind tunnel and the small change of δ with R/ℓ make even a factor of two change in R_D difficult to achieve if, e.g., D/δ were held fixed. Therefore, changes in R/ℓ were utilized, which for a given model, are equivalent to variations in R_D. Two examples of this are shown in Figure 10 for model 2D and M = 2.5 and 3.5. The variation of S/D with R_D for M = 2.5 is typical for all but one of the cylinders: it is nearly monotonic and most of the change occurs at the lower end of the range of R_D. The total change is 15%. This kind of change is known to occur for transitional separation[4], but, from the previous discussion of the sidewall boundary layer, this effect can be ruled out here since the boundary layer is definitely turbulent. At M = 3.5 several types of variations were found including the non-monotonic one shown. This variety in the behavior of S/D is related to the alterations in the flow structure - the number and location of the vortices in the upstream separated flow - as R/ℓ is changed. For the purpose of this paper the most important conclusion is that S/D changes by at most 30% for the maximum allowable variation in R/ℓ.

All of the data presented so far are for cylinders. Most of the literature on this subject reports results for cylinders or fins with a cylindrical leading edge; a variety of shapes representative of protuberances on vehicles have been tested, see Reference 14 and the references

---

14. L. M. Couch, "Flow-Field Measurements Downstream of Two Protuberances on a Flat Plate Submerged in a Turbulent Boundary Layer at Mach 3.49 and 4.44," NASA TN D-5297, July 1969.

therein. We did a limited number of tests using other model shapes and some representative data are shown in Figure 11. In all cases k is the height of the protuberance. D is defined as: the diameter of the hemisphere, the base diameter of the truncated cone, the width of the parallelepiped. The model dimensions are given in Table 1. Relative to the cylinder the results for the other models are understandable in terms of the sweepback effect. The larger k/D for the parallelepiped, compared to the cylinder, would also tend to increase S/D. The surface flow patterns for the other three models are qualitatively the same as those for the small cylinders. Since only one model of each type was tested the significance of the various geometrical parameters cannot be judged.

IV. CORRELATIONS

Eq. (1) shows that, for cylinders, S/D depends on four non-dimensional parameters; for general shapes this number will be five since there is another ratio of lengths to consider. The number of parameters involved and the absence of guidelines from theory make it difficult to obtain engineering estimates of the extent of separation, and underscore the need for correlations of the data. These will be discussed, but only for cylinders.

For large cylindrical obstacles k/δ is eliminated from Eq. (1) by definition. For this case, data from other sources show that S/D does not depend on k/D. This study and others show that the change of S/D with R_D is not very great for either small or large cylinders; see the preceding section. Therefore, for large cylindrical obstacles S/D = f(M), neglecting the variation of S/D with R_D. Model 2D has been shown to be a good approximation to a large protuberance for M = 2.5 and 3.5; we shall assume this to be true for M = 4.0 and 4.5. Then the flagged triangle points on Figure 6 exhibit the function f(M) for $R_D = 3.7 \times 10^5$. For each M, the values of S/D vary with R_D in the unsystematic manner discussed in the last section. This spread, for model 2D, is represented by the vertical bands. An average curve through these bands will yield approximate values of S/D for large cylindrical protuberances.

Westkaemper[5] proposed a correlation for cylinders using a large collection of his own data, obtained by surface indicator methods, and data of others. His conclusions can be questioned because separation was defined differently in the various sources. The treatment of some of the data from other sources was biased, and there is a possible systematic error in his data. These points will be discussed later. He considered only supersonic flow with a turbulent boundary layer and cylindrical protuberances having $k > \delta$. He cautions against using the correlation for cylinders "that do not extend to the outer edge of the boundary layer." This is not the same as requiring the protuberances to

be large according to the definition adopted here; his condition would permit small protuberances. His correlation can be stated analytically as $S/D = 2.65$ for $k/D > 1.13$ and $S/D = 2.42\ (k/D)^{0.7}$ for $k/D < 1.13$ and is shown in Figures 7 and 8. This single relation is supposed to hold for $2 \leq M \leq 20$ and for all R_D provided the boundary layer is turbulent. Data that have appeared after Reference 5 do not support such a simple correlation.

Figures 7 and 8 give an evaluation of Westkaemper's correlation. Our data points designated by squares and triangles and those of References 4 and 12 have $k > \delta$. The disagreement with the correlation is considerable, being more pronounced at $M = 2.5$. For $M = 1.5$, 4.0, and 4.5 our data are consistent with the trend shown in Figures 7 and 8; they agree with the correlation for $M = 4.0$ and lie above it for $M = 4.5$. The correlation gives $S/D = 1.56$, compared to our value, $S/D = .85$, for model 2B at $M = 2.0$ with $k = \delta$. Therefore, even for $k \geq \delta$ this function of one variable can only correlate data if deviations of almost a factor of two are acceptable.

The first reason we question the conclusions of Reference 5 is that in the various sources of data, separation was determined by four different techniques: (i) surface indicator; (ii) noting the first change in a pressure gauge reading from the undisturbed, upstream reading; (iii) same as (ii) but for heat transfer; (iv) extrapolating the separation shock through the boundary layer to the wall. There is no evidence that these techniques give comparable values of S. There are discussions in the literature (Reference 15 being one of the latest) for both two-dimensional and three-dimensional flows which show that (ii) yields a larger S than (i). There are indications that (iii) and (iv) also give values of S larger than (i), but not necessarily the same as (ii). The second reason concerns the data for large cylinders of Reference 12 for which $S/D = 2.0$, using the surface indicator method. These data are not used in Reference 5 but instead a band of larger S values is obtained from the pressure distributions given in Reference 12. Data from some of the other sources quoted in Reference 5 give at least one other point at $S/D = 2.0$. This results in a spread of almost a factor of two because data using techniques (i) and (ii) are intermixed. The third question has to do with a possible systematic error in Westkaemper's own data; he has forty points at $M = 4.9$ and $R/\ell = 38 \times 10^6$/m. The surface flow pattern was visualized in his experiments by injecting a liquid through an orifice upstream of primary separation. A photograph of the pattern shows that a horseshoe vortex from the injection

---

15. G. S. Settles, S. M. Bogdonoff and I. E. Vas, "Incipient Separation of a Supersonic Turbulent Boundary Layer at Moderate to High Reynolds Numbers," AIAA Journal, Vol. 14, No. 1, January 1976, pp. 50-56.

orifice interacts with primary separation; this has been noted by others, see, e.g., Reference 7. The error in S introduced by this interaction is unknown. If the interaction between the orifice vortex and the separated flow acts to decrease S, which is reasonable, then the fact that Westkaemper's values of S/D for M = 4.9 are less than ours for M = 4.0 might be explained.

Our conclusion is that, even for $k \geq \delta$, the correlation of Reference 5 is not adequate because it deviates from the data used in formulating it, plus the more recent data, by almost a factor of two. Evidently there are additional functional dependencies, as mentioned by Westkaemper[5], which were "obscured by the scatter in the test data." The facts that S/D is most (least) sensitive to variations in k/D (R_D) brought out in Reference 5 are important and supported by all the data; these facts will be used in the correlation proposed here.

First the guidelines from inviscid flow are considered. In the last section it was pointed out that, of the four variables in the functional relationship given by Eq. (1), k/D and M are the most important. This can be shown to be reasonable by considering the inviscid flow over the protuberance and the form of the resulting pressure distribution on the flat surface. In such a case there is no separation shock, only a bow shock with detachment distance, Δ. For a large cylindrical protuberance this means that Δ/D is only a function of Mach number. The pressure change across this nearly two-dimensional shock is also independent of k/D; it depends only on M. Thus, the pressure gradient imposed on the boundary layer has the same functional dependence and it is not surprising that S/D depends most strongly on M. For a small cylindrical protuberance, the inviscid flow bow shock position additionally depends on k/D, so that

$$\Delta/D = g(k/D, M).$$

Thus both k/D and M should have a significant effect on S/D. The important geometrical parameters can be identified for other models using this same process.

In our correlation S/D is expressed as a simple function of k/D, for a fixed M. The deviation of the data from the correlation curve is considerably less than that of Reference 5 and our correlation holds even for $k < \delta$.

If the M = 2.50 data shown in Figure 7 are supplemented by those for the other R/ℓ values, then for each k/D a range of values of S/D is obtained. These are shown by bands on Figure 12. The variations in the two parameters are $0.38 \leq k/\delta \leq 4.05$ and $5.6 \leq R_D x 10^{-4} \leq 150$. A function which "fits" these bands is

$$S/D = 2.2\ (1 - e^{-1.25k/D}) \quad .$$

Note that this gives an asymptote of 2.2 whereas there are several data points on Figure 7 showing an asymptote of 2.0. The reason for this is that the extent of the bands, especially for $k/D > 2.0$, is biased by the data point for the lowest R/ℓ. Except for small values of R/ℓ, the data points are essentially at the lower boundary of the band. This is clear from Figure 10, M = 2.5. Therefore, if only large Reynolds numbers are of interest, the curve should be modified for $k/D > 2$ so that it fits the lower bound of the bands. As it is the data depart from the curve by at most 25%; if the lowest value of R/ℓ is excluded the deviation is even less. Treating the data for M = 3.5 in the same way gives the results shown in Figure 13. The average deviation of the data from the curve

$$S/D = 2.3\ (1 - e^{-1.50k/D})$$

is less than for the M = 2.5 case, but the maximum is again 25%. The variations of the two parameters ignored in this correlation are $0.42 \leq k/\delta \leq 4.77$ and $3.5 \leq R_D x 10^{-4} \leq 150$.

We do not have enough data at the other Mach numbers to allow us to present correlations for them but the data we have are consistent with the form of the results for M = 2.5 and 3.5. For large protuberances the correlation discussed previously, see Figure 6, can be used for $M > 3.5$.

V. CONCLUSIONS

In this paper we have concentrated on the upstream separated flow caused by obstacle-boundary layer interaction, specifically the primary separation distance, S. Using the optical-surface indicator technique we determined the surface flow pattern and obtained accurate measurements of S for both large and small protuberances immersed in a supersonic turbulent boundary layer. The data show that S/D is dependent on both k/D and M, but only weakly dependent on Reynolds number. The Reynolds number dependence is related to changes in the flow structure[2]. Further work is required to gain insight into the complex flow in the separated region.

A correlation for S is proposed that holds for both large and small cylindrical obstacles. The correlation is more successful for large cylinders since S scales with D; this is not true for small cylinders. The data used to develop the correlation have values of k/δ that vary by a factor of 10 and values of R_D which vary by a factor of 27 for M = 2.5 and 43 for M = 3.5. A larger number of models and a greater range of parameters would be desirable to achieve a definitive correlation. Two

significant deductions from this work are that S/D can be correlated by the same curve for both large and small cylindrical protuberances and that the data deviate from the correlation curves by no more than 25%.

REFERENCES

1. R. Sedney, "A Survey of the Effects of Small Protuberances on Boundary Layer Flows," AIAA Journal, Vol. 11, No. 6, June 1973, pp. 782-792.

2. R. Sedney and C. W. Kitchens, Jr., "The Structure of Three-Dimensional Separated Flows in Obstacle-Boundary Layer Interactions," AGARD-CP-168, Flow Separation, Paper 37, pp. 1-15. See also BRL Report 1791, Ballistic Research Laboratories, June 1975 (AD A011254).

3. R. H. Korkegi, "Survey of Viscous Interaction Associated with High Mach Number Flight," AIAA Journal, Vol. 9, No. 5, May 1971, pp. 771-784.

4. L. G. Kaufman, R. H. Korkegi and L. C. Morton, "Shock Impingement Caused by Boundary-Layer Separation Ahead of Blunt Fins," AIAA Journal, Vol. 11, No. 10, October 1973, pp. 1363-1364. See also ARL 72-0118, Aerospace Research Laboratories, August 1972.

5. J. C. Westkaemper, "Turbulent Boundary-Layer Separation Ahead of Cylinders," AIAA Journal, Vol. 6, No. 7, July 1968, pp. 1352-1355.

6. R. Sedney, "Visualization of Boundary Layer Flow Patterns Around Protuberances Using an Optical-Surface Indicator Technique," The Physics of Fluids, Vol. 15, No. 12, December 1972, pp. 2439-2441.

7. R. Sedney, C. W. Kitchens, Jr., and C. C. Bush, "Combined Flow Visualization Techniques," AIAA Paper 76-55, AIAA 14th Aerospace Sciences Meeting, Washington, DC, January 1976.

8. C. W. Kitchens, Jr., C. C. Bush and R. Sedney, "Characteristics of the Sidewall and Floor Boundary Layers in BRL Supersonic Wind Tunnel No. 1," BRL Memorandum Report 2563, Ballistic Research Laboratories, December 1975 (AD B008566L).

9. R. L. Maltby, "Flow Visualization in Wind Tunnels Using Indicators," AGARD-ograph 70, AGARD-NATO Fluid Dynamics Panel, 1962.

10. E. A. Price and R. L. Stallings, "Investigation of Turbulent Separated Flows in the Vicinity of Fin-Type Protuberances at Supersonic Mach Numbers," NASA TN D-3804, February 1967.

11. D. R. Chapman, D. M. Kuehn and H. K. Larson, "Investigation of Separated Flows in Supersonic and Subsonic Streams with Emphasis on the Effect of Transition," NACA Report 1356, 1958.

12. D. M. Voitenko, A. I. Zubkov and Y. A. Panov, "Supersonic Gas Flow Past a Cylindrical Obstacle on a Plate," Mekhanika Zhidkosti i Gaza, Vol. 1, No. 1, 1966, pp. 121-125.

13. A. E. Winklemann, "Flow Visualization Studies of a Fin Protuberance Partially Immersed in a Turbulent Boundary Layer at Mach 5," NOLTR 70-93, Naval Ordnance Laboratory, May 1970.

14. L. M. Couch, "Flow-Field Measurements Downstream of Two Protuberances on a Flat Plate Submerged in a Turbulent Boundary Layer at Mach 3.49 and 4.44," NASA TN D-5297, July 1969.

15. G. S. Settles, S. M. Bogdonoff and I. E. Vas, "Incipient Separation of a Supersonic Turbulent Boundary Layer at Moderate to High Reynolds Numbers," AIAA Journal, Vol. 14, No. 1, January 1976, pp. 50-56.

LIST OF SYMBOLS

h	height of oil streak used in the optical-surface indicator technique, m
k	height of the obstacle (see Table 1), m
p_o	wind tunnel stagnation pressure, cm-Hg absolute
A	indicates the position of attachment line in flow symmetry plane in Figure 3
B	indicates the bow shock position in Figure 3
D	diameter of the obstacle (see Table 1), m
M	free-stream Mach number, nondimensional. Also used to indicate the Mach stem position in Figure 3.
R/ℓ	unit Reynolds number ($= U/\nu$), m^{-1}
R_D	Reynolds number based on obstacle diameter ($= UD/\nu$), nondimensional
R_k	Reynolds number based on obstacle height and U_k ($= U_k k/\nu$), nondimensional
S	primary separation distance, measured from the obstacle leading edge to the most upstream position of primary separation, m
S_∞	value of S for an "infinite effective height" cylinder of the same diameter, m
U	free-stream velocity, m/s
U_k	undisturbed velocity at the height k off the surface, m/s
V	indicates the position of a vortex core in Figure 3
δ	99% velocity boundary-layer thickness, m
Δ	bow shock detachment distance in flow symmetry plane, m

CYLINDERS

		A	B	C	D
1	k D	1.02 1.91	2.03 1.91	4.06 1.91	10.16 1.91
2	k D	1.02 3.81	2.03 3.81	4.06 3.81	10.16 3.81
3	k D	1.02 7.62	2.03 7.62	4.06 7.62	
4	k D	1.91 HEMISPHERE 3.81			
5	k D	2.03 TRUNCATED CONE 3.81 (Base) 1.91 (Top)			
6	k	2.03 PARALLELEPIPED 2.54 (Width) 2.03 (Depth)			

Table 1. Model dimensions (cm), designation (e.g., 2C) and plotting symbols used on graphs

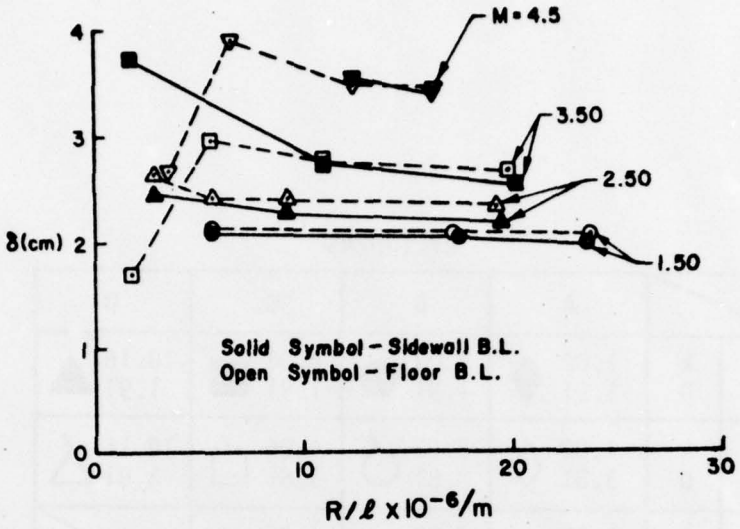

Figure 1. Boundary-Layer Thickness (δ) vs. Unit Reynolds Number from Pitot Surveys

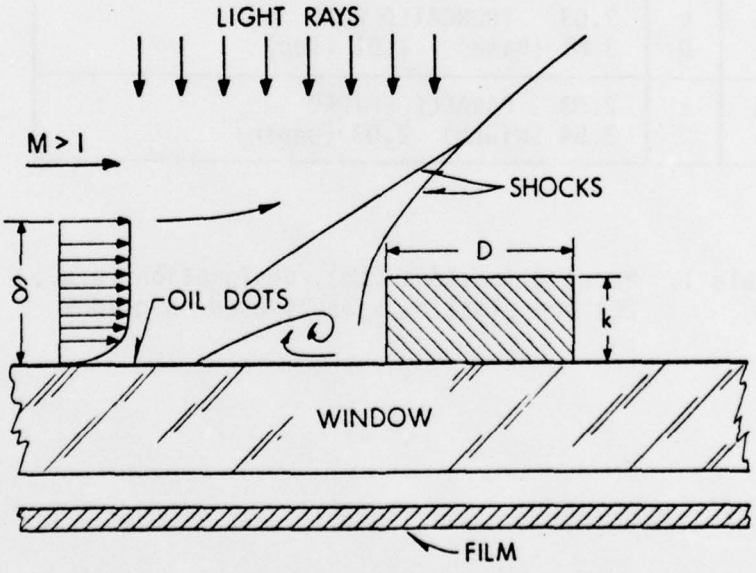

Figure 2. Schematic of Optical-Surface Indicator Technique Showing Small Protuberance Immersed in Supersonic Turbulent Boundary Layer

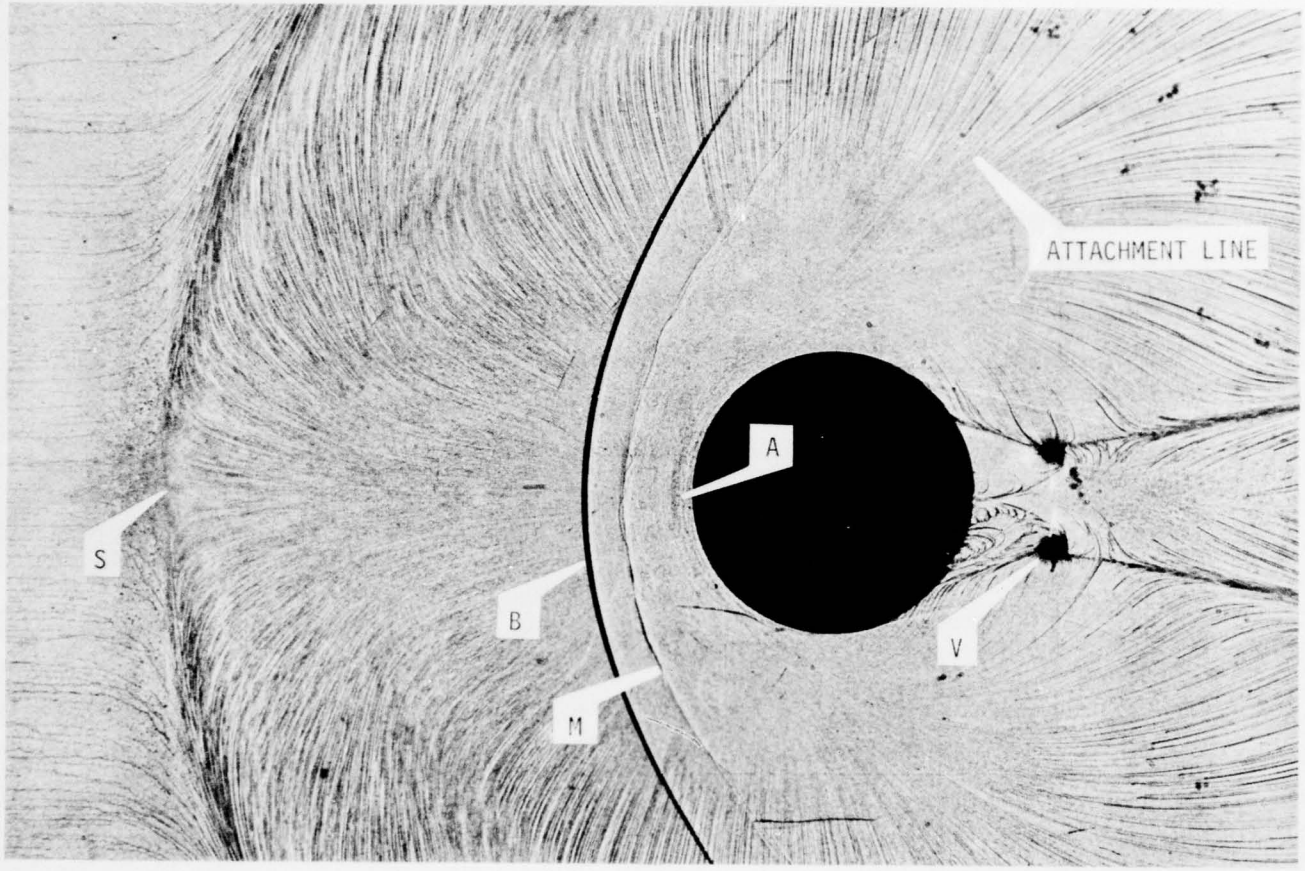

Figure 3. Plan-View Shadowgraph for Large Protuberance, Model 2D, $M = 2.50$, $R/\ell = 19.3 \times 10^6/m$. S - Primary Separation, B - Bow Shock, M - Mach Stem, A - Attachment Line, V - Vortex Core. Attachment Line Indicated Originates at Point A

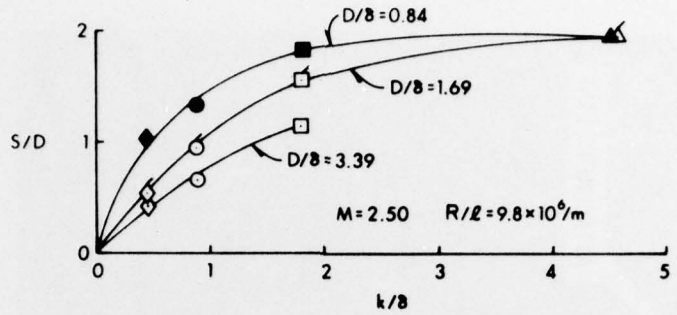

Figure 4. Primary Separation Distance (S/D) vs. Protuberance Height (k/δ), δ = 2.25 cm

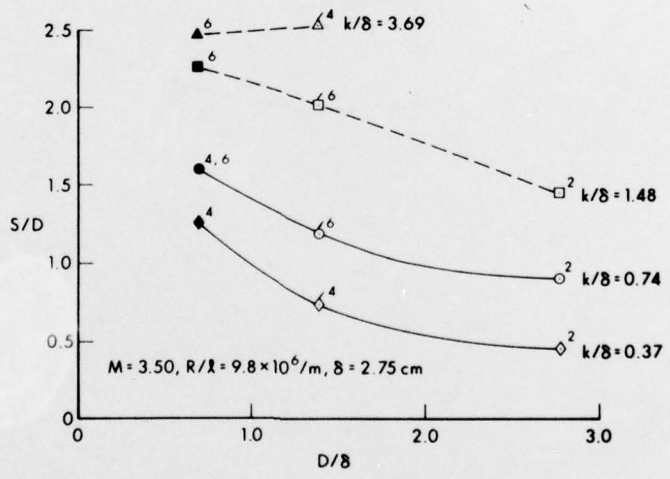

Figure 5. Primary Separation Distance (S/D) vs. Protuberance Diameter (D/δ)

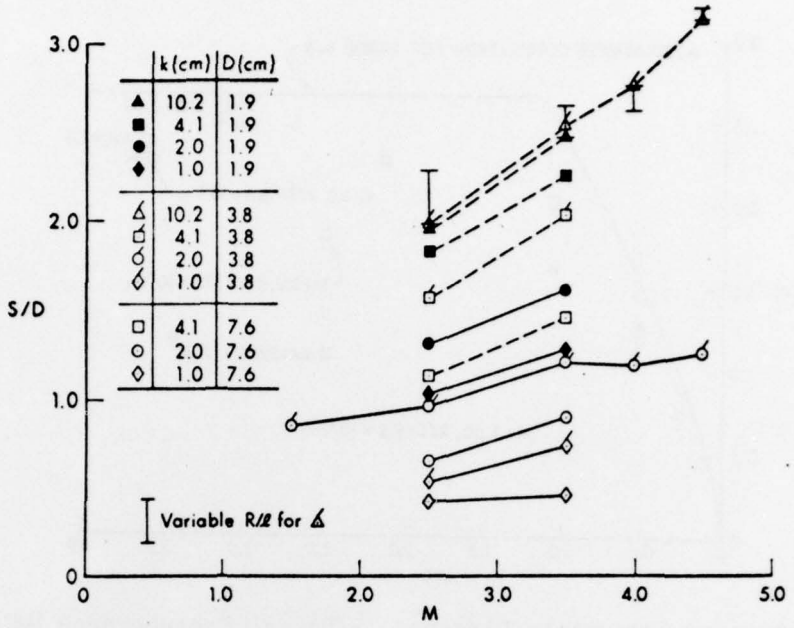

Figure 6. Primary Separation Distance (S/D) vs. Mach Number (M), $R/\ell = 9.8 \times 10^6/m$

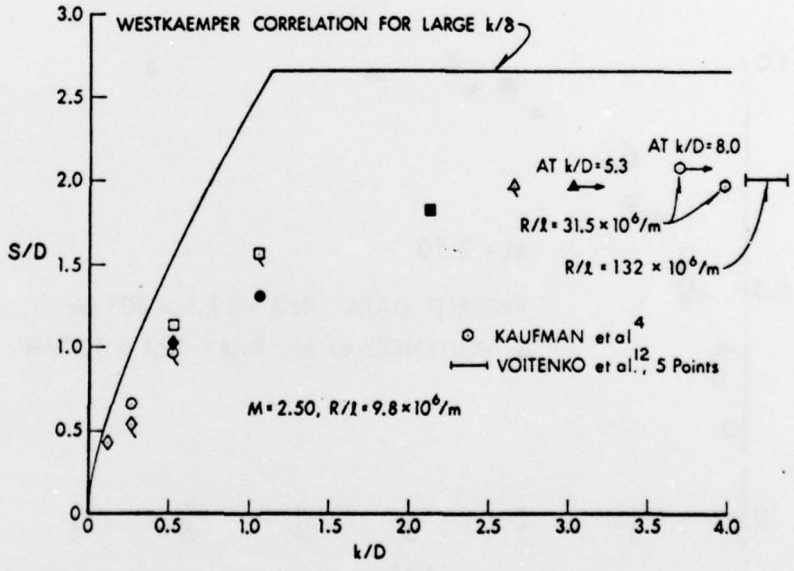

Figure 7. Primary Separation Distance (S/D) vs. Protuberance Height (k/D) $\delta = 2.25$ cm

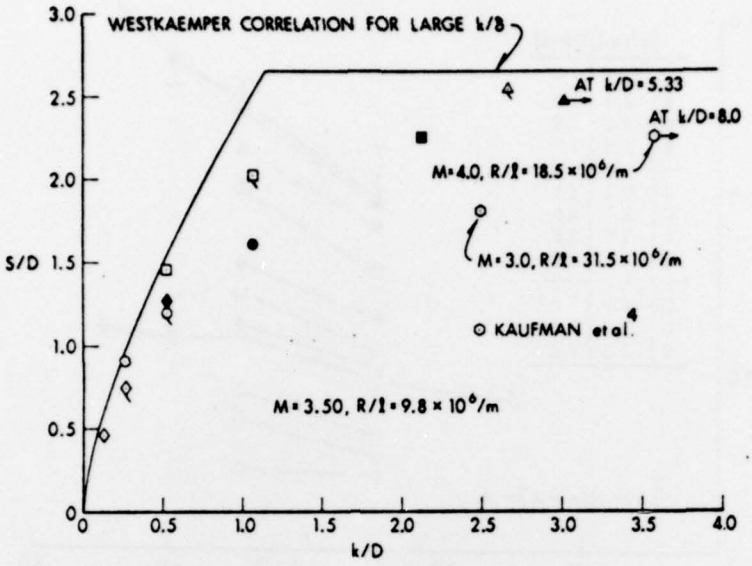

Figure 8. Primary Separation Distance (S/D) vs. Protuberance Height (k/D)
δ = 2.75 cm

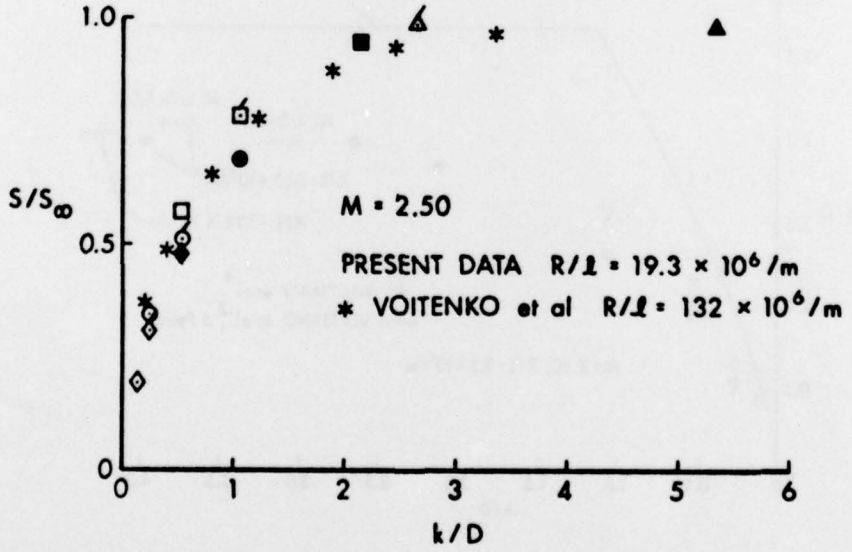

Figure 9. Primary Separation Distance (S/S_∞) for Finite Height Cylinders vs. Protuberance Height (k/D)

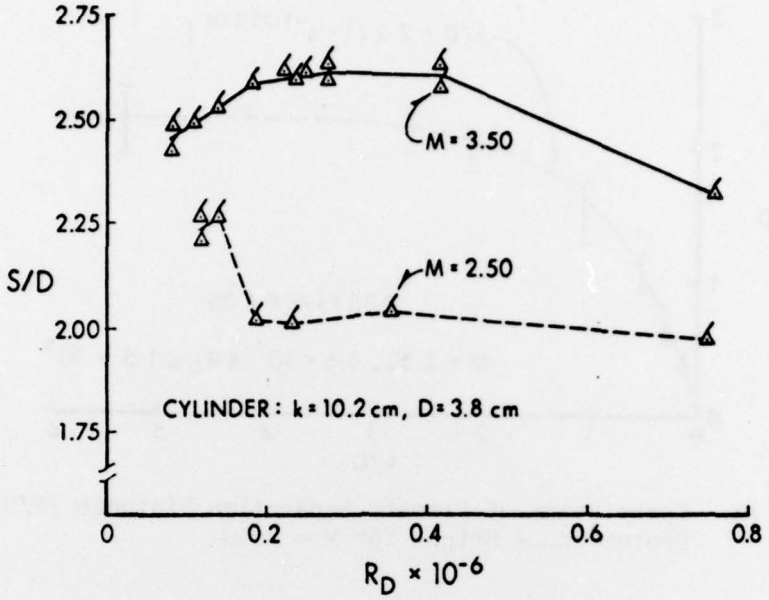

Figure 10. Primary Separation Distance (S/D) vs. Reynolds Number (R_D) for Cylinder Model 2D

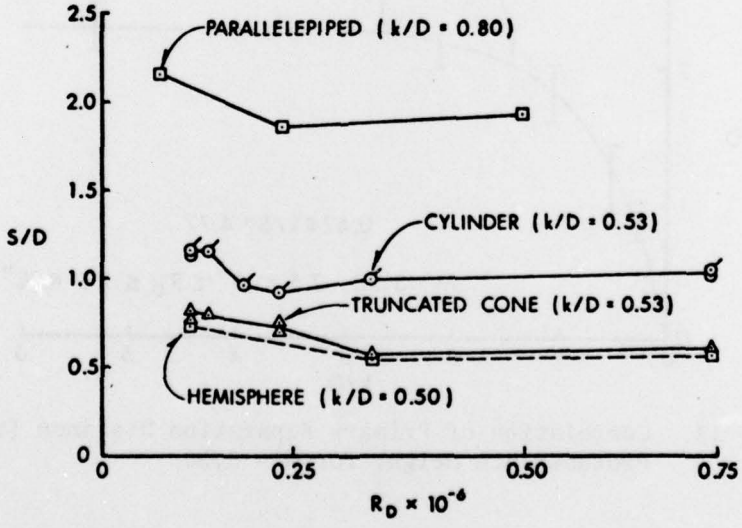

Figure 11. Variation of Primary Separation Distance (S/D) with Reynolds Number (R_D) for Four Protuberance Shapes

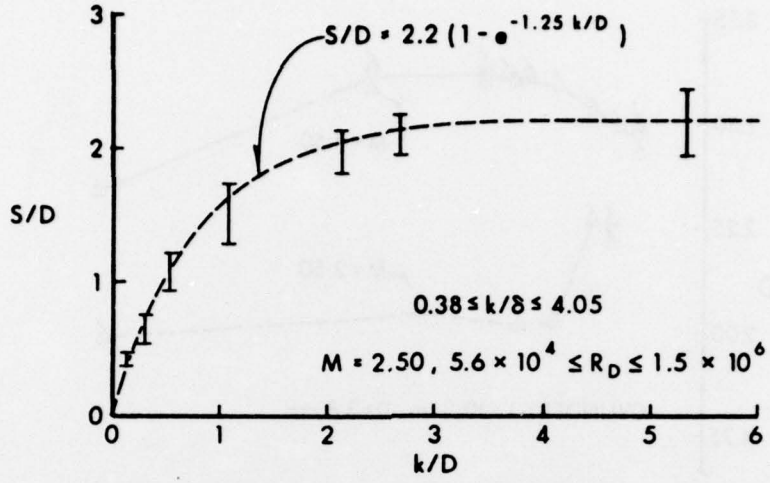

Figure 12. Correlation of Primary Separation Distance (S/D) vs. Protuberance Height for M = 2.50

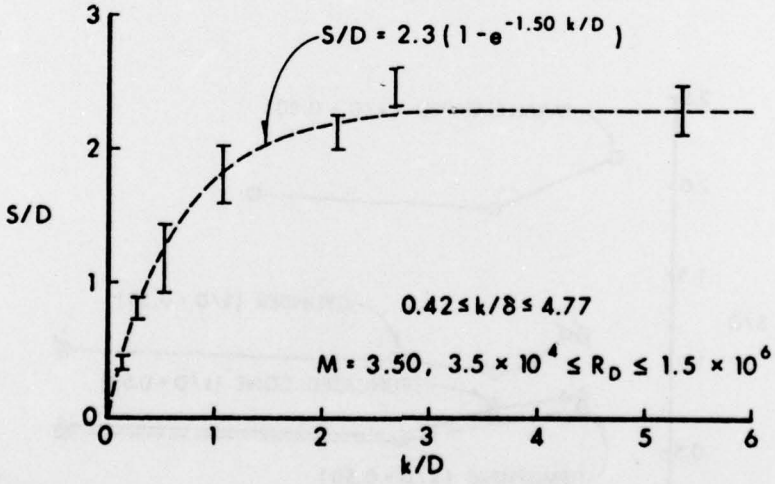

Figure 13. Correlation of Primary Separation Distance (S/D) vs. Protuberance Height for M = 3.50

DISTRIBUTION LIST

No. of Copies	Organization
12	Commander Defense Documentation Center ATTN: DDC-TCA Cameron Station Alexandria, VA 22314
1	Commander US Army Materiel Development and Readiness Command ATTN: DRCDMA-ST 5001 Eisenhower Avenue Alexandria, VA 22333
1	Commander US Army Aviation Systems Command ATTN: DRSAV-E 12th and Spruce Streets St. Louis, MO 63166
1	Commander US Army Air Mobility Research and Development Laboratory Ames Research Center Moffett Field, CA 94035
1	Commander US Army Electronics Command ATTN: DRSEL-RD Fort Monmouth, NJ 07703
2	Commander US Army Missile Command ATTN: DRSMI-R Ray Deep Redstone Arsenal, AL 35809
1	Commander US Army Tank Automotive Development Command ATTN: DRDTA-RWL Warren, MI 48090
2	Commander US Army Mobility Equipment Research & Development Command ATTN: Tech Docu Cen, Bldg. 315 DRSME-RZT Fort Belvoir, VA 22060
1	Commander US Army Armament Command Rock Island, IL 61202
1	Commander US Army Picatinny Arsenal ATTN: SARPA-FR-S-A, A. Loeb Dover, NJ 07801
1	Commander US Army Harry Diamond Labs ATTN: DRXDO-TI 2800 Powder Mill Road Adelphia, MD 20783
1	Director US Army TRADOC Systems Analysis Activity ATTN: ATAA-SA White Sands Missile Range NM 88002
1	AGARD-NATO ATTN: R. H. Korkegi APO New York 09777
3	Commander US Naval Air Systems Command ATTN: AIR-604 Washington, DC 20360
3	Commander US Naval Ordnance Systems Command ATTN: ORD-0632 ORD-035 ORD-5524 Washington, DC 20360

DISTRIBUTION LIST

No. of Copies	Organization
2	Commander David W. Taylor Naval Ship Research & Development Center ATTN: Tech Library S. de los Santos Head, High Speed Aero Div Bethesda, MD 20084
4	Commander US Naval Surface Weapons Center Applied Aerodynamics Division ATTN: Code 312 K. Lobb S. M. Hastings A. E. Winklemann W. C. Ragsdale Silver Spring, MD 20910
1	Commander US Naval Surface Weapons Center ATTN: Tech Library Dahlgren, VA 22448
1	AFATL (DLDL, Dr. D.C. Daniel) Eglin AFB, FL 32542
2	AFFDL (W. L. Hankey; J.S.Shang) Wright-Patterson AFB, OH 45433
5	Director National Aeronautics and Space Administration ATTN: J. Rakich J. Marvin B. Wick D. R. Chapman Tech Lib Ames Research Center Moffett Field, CA 94035
6	Director National Aeronautics and Space Administration Langley Research Center ATTN: D. Bushnell R. Trimpi J. South E. Price J. R. Sterrett Tech Lib Langley Station Hampton, VA 23365
1	Director National Aeronautics and Space Administration Lewis Research Center ATTN: MS 60-3, Tech Lib 21000 Brookpark Road Cleveland, OH 44135
1	Director National Aeronautics and Space Administration Marshall Space Flight Center ATTN: A. R. Felix, Chief S&E-AERO-AE Huntsville, AL 35812
2	Director Jet Propulsion Laboratory ATTN: J. Kendall Tech Lib 4800 Oak Grove Drive Pasadena, CA 91103
3	ARO, Inc. ATTN: J. D. Whitfield R. K. Matthews Tech Lib Arnold AFB, TN 37389

DISTRIBUTION LIST

No. of Copies	Organization
2	Aerospace Corporation ATTN: H. Mirels R. L. Varwig Aerophysics Lab P. O. Box 92957 Los Angeles, CA 90009
1	AVCO Systems Division ATTN: B. Reeves 201 Lowell Street Wilmington, MA 01887
1	The Boeing Company Commercial Airplane Group ATTN: W. A. Bissell, Jr. M. S. 1W-82, Org 6-8340 Seattle, WA 98124
2	Calspan Corporation ATTN: A. Ritter M. S. Holden P. O. Box 235 Buffalo, NY 14221
1	Center for Interdisciplinary Programs ATTN: Victor Zakkay W. 177th St. & Harlem River Bronx, NY 10453
1	General Dynamics ATTN: Research Lib 2246 P. O. Box 748 Fort Worth, TX 76101
1	General Electric Company ATTN: H. T. Nagamatsu Research & Development Lab (Comb. Bldg.) Schenectady, NY 12301
2	Grumman Aerospace Corporation ATTN: R. E. Melnik L. G. Kaufman Research Department Bethpage, NY 11714
2	Lockheed-Georgia Company ATTN: B. H. Little, Jr. G. A. Pounds Dept 72074, Zone 403 86 South Cobb Drive Marietta, GA 30062
1	Lockheed Missiles and Space Company ATTN: Tech Info Center 3251 Hanover Street Palo Alto, CA 94304
4	Martin-Marietta Laboratories ATTN: S. H. Maslen S. C. Traugott P. Jordan H. Obremski 1450 S. Rolling Road Baltimore, MD 21227
2	McDonnell Douglas Astronautics Corporation ATTN: J. Xerikos H. Tang 5301 Bolsa Avenue Huntington Beach, CA 92647
1	McDonnell Douglas Research Laboratories ATTN: R. Hakkinen Manager - Research Flight Sciences Dept 222, Bldg. 33 P. O. Box 516 St. Louis, MO 63166

DISTRIBUTION LIST

No. of Copies	Organization
1	Northrup Corporation Aircraft Division ATTN: S. Powers 3901 West Broadway Hawthorne, CA 90250
1	Sandia Laboratories ATTN: Tech Lib P. O. Box 5800 Albuquerque, NM 87115
1	United Aircraft Corporation Research Laboratories ATTN: Library East Hartford, CT 06108
1	Vought Systems Division LTV Aerospace Corporation ATTN: J. M. Cooksey Chief, Gas Dynamics Lab., 2-53700 P. O. Box 5907 Dallas, TX 75222
1	California Institute of Technology Guggenheim Aeronautical Lab ATTN: Tech Lib Pasadena, CA 91104
1	Cornell University Graduate School of Aero Engr ATTN: Library Ithaca, NY 14850
2	Illinois Institute of Tech ATTN: M. V. Morkovin H. M. Nagib 3300 South Federal Chicago, IL 60616
1	Massachusetts Institute of Technology ATTN: Tech Library 77 Massachusetts Avenue Cambridge, MA 02139
2	North Carolina State University Mechanical and Aerospace Engineering Department ATTN: F. F. DeJarnette J. C. Williams Raleigh, NC 27607
1	Notre Dame University ATTN: T. J. Mueller Dept of Aero Engr South Bend, IN 46556
2	Ohio State University Department of Aeronautical & Astronautical Engineering ATTN: S. L. Petrie Tech Lib Columbus, OH 43210
1	Princeton University Dept of Aerospace & Mechanical Sciences ATTN: S. I. Cheng Princeton, NJ 08540
3	Princeton University James Forrestal Research Center Gas Dynamics Laboratory ATTN: I. E. Vas S. M. Bogdonoff Tech Lib Princeton, NJ 08540
1	Rutgers University Dept of Mechanical, Industrial and Aerospace Engineering ATTN: R. H. Page New Brunswick, NJ 08903
1	Southern Methodist University Dept of Civil & Mechanical Engineering ATTN: R. L. Simpson Dallas, TX 75275

DISTRIBUTION LIST

No. of Copies	Organization
1	Southwest Research Institute Applied Mechanics Reviews 8500 Culebra Road San Antonio, TX 78228
1	University of California - Berkley Dept of Aerospace Engineering ATTN: M. Holt Berkeley, CA 94720
1	University of California - San Diego Department of Aerospace and Mechanical Engr Sciences ATTN: Tech Lib La Jolla, CA 92037
1	University of Colorado Dept of Astro-Geophysics ATTN: E. R. Benton Boulder, CO 80302
2	University of Maryland ATTN: W. Melnik Tech Lib College Park, MD 20740
1	University of Michigan Department of Aeronautical Engineering ATTN: Tech Lib East Engineering Building Ann Arbor, MI 48104
1	University of Santa Clara Department of Physics ATTN: R. Greeley Santa Clara, CA 95053
1	University of Texas Dept of Aerospace Engineering ATTN: J. C. Westkaemper Austin, TX 78712
1	University of Virginia Dept Aerospace Engineering & Engineering Physics ATTN: Tech Lib Charlottesville, VA 22904
1	University of Washington Dept of Mechanical Engineering ATTN: Tech Lib Seattle, WA 98195
1	Virginia Polytechnic Institute Dept of Aerospace Engineering ATTN: G. R. Inger Blacksburg, VA 24061
	Aberdeen Proving Ground
	Marine Corps Ln Ofc Dir, USAMSAA


FILM
4